

Journal of Materials Chemistry B

Accepted Manuscript



This is an *Accepted Manuscript*, which has been through the Royal Society of Chemistry peer review process and has been accepted for publication.

Accepted Manuscripts are published online shortly after acceptance, before technical editing, formatting and proof reading. Using this free service, authors can make their results available to the community, in citable form, before we publish the edited article. We will replace this *Accepted Manuscript* with the edited and formatted *Advance Article* as soon as it is available.

You can find more information about *Accepted Manuscripts* in the [Information for Authors](#).

Please note that technical editing may introduce minor changes to the text and/or graphics, which may alter content. The journal's standard [Terms & Conditions](#) and the [Ethical guidelines](#) still apply. In no event shall the Royal Society of Chemistry be held responsible for any errors or omissions in this *Accepted Manuscript* or any consequences arising from the use of any information it contains.

Cite this: DOI: 10.1039/c0xx00000x

ARTICLE TYPE

www.rsc.org/xxxxxx

Fast setting and anti-washout injectable calcium–magnesium phosphate cement for minimally invasive treatment in bone defect

Fangping Chen^{a,b,c}*, Zhiyan Song^c and Changsheng Liu^{a,b,c,*}

Received (in XXX, XXX) XthXXXXXXXXXX 20XX, Accepted Xth XXXXXXXXXXXX 20XX

DOI: 10.1039/b000000x

The development of injectable calcium phosphate cements (ICPC) represents a promising approach for minimally invasive surgical techniques. However, the undesirable anti-washout property and slow setting time of ICPC greatly hamper its clinical application. Xanthan gum (XG) has strong hydrophilic, shape retention and rheological property. In this study, a fast setting and anti-washout injectable calcium–magnesium phosphate cement (fa-ICMPC) was developed by introducing XG as an anti-washout agent and MPC into CPC. The bone-regenerative capacity and the bioresorption of the fa-ICMPC were also investigated by injecting directly to a rabbit thighbone defect. The result showed that XG imparted anti-washout to the fa-ICMPC and enhanced the injectability of the fa-ICMPC. With the protection of thick viscous films formed by XG, the setting of the fa-ICMPC was not disturbed but accelerated with the synergistic effect of MPC. The result demonstrated that fa-ICMPC was not crumbled and could be filled the defects tightly. The newly formed bone tissue grew into the fa-ICMPC along with the degradation of the materials. In short, the fa-ICMPC exhibited potent anti-washout property, fast setting, improved injectability, good biodegradability and osteoconductivity, and has potential application to repair the bone defects by minimally invasive treatment.

Introduction

Due to the increasing population-ageing, inflammatory disease, trauma and congenital conditions, bone fractures are becoming progressively a common medical problem. With the growing demand of minimally invasive techniques in surgical procedures, injectable biomaterials are widely researched with advantages of filling irregularly shaped bone cavity, being injected into bone defects without open surgery, shorter hospitalization periods, reduced pain and risk of postoperative infection for the patient.^{1,2} Currently, the most commonly used injectable bone cement is

poly (methyl methacrylate) (PMMA), but it suffers from the fact that it is not degraded and its high curing temperature tends to cause necrosis of the surrounding tissue.

Injectable calcium phosphate cement (ICPC) is an attractive candidate because of the unique combination of self-setting under ambient temperature, conformity to the shape of bone defects, and biodegradability. However, the setting time of ICPC is longer than the conventional CPC because of its higher ratio of liquid to powder. In addition, the existence of ions and organic compounds in plasma or tissue fluid would suppress or delay the hydroxyapatite (HAP) formation from the dissolved cement, which also prolonged the setting time³. The two factors above made the ICPC crumble upon early contact with blood or other tissue fluid. A strong washout resistance is an important attribute for injectable biomaterials because excessive amounts of fluid are often present at the surgical site. Therefore, it is necessary to develop an excellent anti-washout property and fast setting ICPC while maintaining its injectability.

Acceleration the setting process and immobilizing the particles in ICPC is an effective method to improve the anti-washout property. Magnesium phosphate cement (MPC) is a new type of cement with rapid setting and high initial mechanical strength. MPCs were set in 7-15 min to form magnesium

^aThe State Key Laboratory of Bioreactor Engineering, East China University of Science and Technology, Shanghai 200237, PR China. Fax: 86-21-64251358; Tel.:86-21-64251308; E-mail: fpchen@ecust.edu.cn

^bKey Laboratory for Ultrafine Materials of Ministry of Education, School of Materials Science and Engineering, East China University of Science and Technology, Shanghai 200237, PR China

^cEngineering Research Center for Biomedical Materials of Ministry of Education, East China University of Science and Technology, Shanghai 200237, PR China

phosphate ($\text{Mg}_3(\text{PO}_4)_2$) and calcium triphosphate ($\text{Ca}_3(\text{PO}_4)_2$) as the final products, and had a compressive strength of 35 MPa after setting for 30 min.^{4,5} Studies also revealed that the addition of MPC could regulate the setting time and improve the setting strength of ICPC effectively.^{6,7,8} Considering this, the addition of MPC is an effective way to prevent the disintegration of ICPC.

Xanthan gum (XG) is a water-soluble anionic polysaccharide produced by *Xanthomonas campestris*. It is nontoxic and biocompatible, and has been approved by FDA as an unlimited food additive since 1969. With a large number of hydrophilic groups, XG has strong hydrophilic and shape retention. In addition, XG is used as a rheological control agent in industries and as a stabilizer for emulsions and suspensions.⁹ These advantages of xanthan gum motivated us to hypothesize that the incorporation of XG may improve the anti-washout property of the injectable biomaterial while preserving its fast setting and injectability. For this purpose, a fast setting and anti-washout injectable calcium–magnesium phosphate cement (fa-ICMPC) was developed by introducing XG and MPC into CPC in this study.

However, to our knowledge, few injectable biomaterials have been injected directly to the defect and evaluated *in vivo*. An injectable decalcified bone matrix (DBM)/glycerol biocomposite were reported to heal rabbit calvaria critical-size defects after 12 weeks.¹⁰ However, it had weak mechanical properties and did not provide immediate protection since the material was non-settable. Yu et al investigated the *in vivo* performance of injectable CPC–bioglass (BG) composite. The *in vivo* results showed that CPC–BG enhanced the new bone formation in rabbits' femoral defect.¹¹ However, the CPC–BG was implanted in block not injected in the defect, so its anti-washout property was not involved. In addition, the *in vivo* bone regeneration and bioresorption have not been reported so far. Therefore, the aim of this study was first to develop a new type of fa-ICMPC, and second to investigate the osteogenic property and degradability by injecting fa-ICMPC to the rabbit thighbone defect.

Experimental

Preparation of fa-ICMPC and ICPC

CPC powders were composed of tetracalcium phosphate (TTCP) and dicalcium phosphate anhydrous (DCPA) in an equivalent molar ratio. TTCP was synthesized by a solid-to-solid reaction between calcium phosphate and calcium carbonate at 1500 °C for 8 h. DCPA was obtained by removing the crystallization water in dicalcium phosphate dihydrate (DCPD) at 120 °C. DCPD was prepared from $(\text{NH}_4)_2\text{HPO}_4$ and $\text{Ca}(\text{NO}_3)_2$ in an acidic environment. All calcium phosphates were prepared in our laboratory, and the preparation method was in accordance with the relevant literature.¹² MPC powders are composed of MgO and $\text{Ca}(\text{H}_2\text{PO}_4)_2$ in a molar ratio of 2:1. Magnesium carbonate basic pentahydrate [$\text{MgCO}_3 \cdot 4\text{Mg}(\text{OH})_2 \cdot 5\text{H}_2\text{O}$] was sintered at 1500 °C for 6 h to form the MgO. After cooling to room temperature, the powders were ground for 5 min and sieved to obtain particles less than 74 μm in diameter. The mixed MPC powders were kept in a desiccator for further experiment.

The c-ICPC consisted of pure CPC powders and deionized

water at the fixed ratio of 2 g/mL. The injectable calcium–magnesium phosphate cements (ICMPC) consist of powder phase and liquid phase. The ICMPC powders were prepared by mixing CPC with MPC powders in an equivalent weight ratio. The c-ICMPC was formed by mixing the CMPC powders with deionized water at the fixed ratio of 2 g/mL.

1.0 wt% Xanthan gum (Mingzhu Biotechnology Science & Technology Co., Ltd, China) solution was used as the liquid phase of the fa-ICMPC. The fa-ICMPC paste was formed by mixing the CMPC powders with the XG solution with a spatula at 2 g/mL homogeneously. Except the XG, all the other chemicals were purchased from Sinopham Chemical Reagent Co., Ltd. Shanghai, China.

Anti-washout Evaluation

The homogeneous paste of c-ICPC, c-ICMPC and fa-ICMPC were transferred to a 2.5 mL disposable syringe with a nozzle inner diameter of 5.0 mm. The paste was extruded by the syringe into the deionized water and shaken at 100 rpm for 5 min at 37 °C. The anti-washout of the cement was evaluated visibly by the extent of disintegration of the pastes.¹³ Quantitative measurements of the washout mass loss rate of the paste were not done considering the exchange of the solutions.¹⁴

Injectability and Setting time

The c-ICPC, c-ICMPC and fa-ICMPC were prepared with P/L ratios ranging from 0.4 to 0.7 mL/g. The injectability of the paste was measured according to the method described by Leonardo et al.¹⁵ A homogeneous paste was formed by mixing 3 min with a spatula, and then transferred into the 2.5 mL disposable syringe with a nozzle diameter of 5.0 mm for injectability measurement. When a 3 kg compressive load was put vertically on the top of the plunger, the paste was extruded through the syringe. The percentage of injectability was calculated by the weight of the paste extruded through the syringe divided by the original weight of the paste in the syringe. Each test was performed three times and the average value was calculated.

The c-ICPC, c-ICMPC and fa-ICMPC pastes were placed into the glass tubes ($\Phi 6 \times 10 \text{ mm}^3$). The top and bottom surfaces of the tube were tightly covered with two sheets of plastic film held by a 'C' clamp. The tube with fa-ICMPC was immersed in deionized water directly and then kept in a 100% relative humidity environment at 37 °C. The tubes with c-ICPC and c-ICMPC were stored in a 100% relative humidity chamber at 37 °C for setting.

According to the ASTM Test Method C 187-98, the setting time was measured by a Vicat apparatus. The Vicat apparatus consists of a frame bearing a movable rod (300 g in mass) and with a stainless steel needle (1 mm in diameter) fitted at the end.^{6,16} The cement samples were removed once every 0.5 min from the 100% relative humidity environment and centered under the 1 mm end of the needle. The rod was lowered vertically on the cement surface. The cement is considered to complete setting when the length of the needle penetrated into the cement less than 1 mm. The time interval from the paste being immersed in the water to the paste completed setting was taken as the setting time. Each experiment was performed five times and the average value

was calculated.

Compressive strength

After setting for 24 h, the hardened cement ($\Phi 6 \times 10 \text{ mm}^3$) was removed from the glass tube and polished uniformly on both sides. The compressive strength of the cement was measured with a universal testing machine (AG-2000A, Shimadzu Autograph, Shimadzu Co. Ltd., Japan) at a loading rate of $1 \text{ mm} \cdot \text{min}^{-1}$. Three replicates were carried out for each group, and the results were expressed as means \pm standard deviation (means \pm SD).

Soaking in simulated body fluid

The simulated body fluid (SBF) was prepared and buffered at pH 7.4 with tris-(hydroxymethyl)-aminomethane $[(\text{CH}_2\text{OH})_3\text{CNH}_2]$ and hydrochloric acid (HCl). The bioactivity in vitro was tested by soaking the c-ICPC, c-ICMPC and fa-ICMPC in SBF at a weight-to-volume rate of 0.2 g/mL at 37°C to monitor the HA formation with time. After soaking for 24 h, all samples were gently rinsed with deionized water, soaked in liquid nitrogen for 15 min to stop the reaction, and dried by freezing over night.

The phase composition of the hardened samples was characterized by X-ray diffraction (XRD, D/max 2550 VB/PC, Rigaku) in a continuous scan mode. The surface morphology of the samples after immersion in SBF was observed by scanning electronic microscopy (SEM, H-800, Hitachi, Japan) at a high magnification with an acceleration voltage of 15 kV .

Animal experiment

Before animal surgery, the samples were sterilized by ethylene oxide. All procedures were approved by the sixth People's Hospital Affiliated with Shanghai Jiao Tong University Committee on the Use and Care of Animals. Six healthy adult New Zealand white rabbits (Silaike Inc. Shanghai, China) were older than 3 months and weighed between 2.6 kg and 2.8 kg . All animals were fasted 24h before assay. All the animals were anesthetized with xylazine (0.02 g/kg) and ketamine (0.1 g/kg). The left thighbone of each rabbit was exposed and the cavitory defects (5 mm in diameter and 5 mm in depth) were created with a medium speed bur. After the defects were washed with physiological saline, the c-ICMPC and fa-ICMPC paste were injected ($n=3$ rabbit/batch) into the defects by the syringe with a needle of 8 mm inner diameter. The incision was closed in layers using absorbable sutures. Prophylactic antibiotic was given for 3 days.

The animals were sacrificed by an overdose abdominal injection of pentobarbital sodium at 1month, 2 months and 3 months after surgery, and the defects with an additional 2-mm surrounding tissue were dissected from the host bone. All the harvested samples were fixed in a 4% paraformaldehyde solution buffered by 0.1 M phosphate solution (pH 7.2) for 3-5 days before further analysis.

Radiographic examination

The harvested bone specimens at 1month, 2 months and 3 months were examined by x-ray machine (WDM, China) at 46 KV and 100 mA with an integration time of 40 ms , to evaluate new bone formation in the bone defects.

Synchrotron Radiation Computed Tomography measurement

To explore the microstructure of injectable cement and to evaluate the repair process for the bone defects, Synchrotron Radiation Computed Tomography (SR-CT) measurement was performed at beamline BL13W of SSRF (Shanghai, China) using a monochromatic beam with an energy of 30 keV and a sample-to-detector distance of 1.5 m . In the current study, a 4000×2500 CCD detector with the pixel size set to 6 mm was used to record images. One thousand two hundred projections within an angular range of 180° were taken and the exposure time amounted to 8 s per projection. 3D structure was reconstructed using a filtered back-projection algorithm. The images were finally redigitized with an 8-bit data format, proportional to the measured attenuation coefficients of the voxels. The VG Studio MAX 2.0 software (Volume Graphics, Heidelberg, Germany) served for the visualization of the tomographic data.

Histological analysis

To determine the amount of newly formed bone quantitatively, the histological sections were analyzed statistically at the end of each implantation period. After fixation with 4% neutral buffered formalin for 48 h, the extracted femora were decalcified in 12.5% EDTA, dehydrated in a graded series of alcohol, and embedded in paraffin. Three sections, representing the central area of each defect, were used for the histometric analysis. The specimens were cut in 150 mm thick sections using a microtome (Leica, Hamburg, Germany) and were subsequently polished to a final thickness of about $4 \mu\text{m}$.¹⁷ After hematoxylin and eosin and Masson trichrome staining, each section was observed with a light microscope under $20\times$ and $100\times$ magnifications. Using image analytical software Image-Pro Plus (Media Cybernetics, USA), new bone volume was expressed as a percentage of the newly formed bone area within the original drill defect area according to the following equation:
New bone volume = (new bone area / original drilled defect area) $\times 100\%$.

Statistical analysis

Statistical analysis was conducted using one-way ANOVA with post hoc tests. The results were expressed as the mean \pm standard deviation. A value of $p < 0.05$ was considered to be statistically significant.

Results and discussion

A major drawback of orthopedic implant materials in current use is their hardened form, which requires the surgeon to drill the surgical site around the graft or to carve the implant into the desired shape and often leads to longer hospitalization periods, increased bone loss, trauma and pain and risk of postoperative infection for the patient.¹⁸ Injectable cements are gaining increasing interest in the orthopedic field, as they can be delivered to the target site via a minimally invasive manner. However, most of the injectable cements are limited in clinic because of their disintegration in blood or other fluids, prolonged setting time and incomplete injectability. In addition, the bone regeneration and bioresorption of ICPC by injecting into the defect have not been reported. Here, in this study, we fabricated the fa-ICMPC by addition XG and MPC to CPC, and investigated

the osteogenesis and biodegradability of fa-ICMPC by injected into the bone defect directly.

Anti-washout property

The anti-washout property is important for injectable cements to use *in vivo*. Some studies have demonstrated that gelling agents such as hydroxypropyl methylcellulose, carboxymethylcellulose, lactic acid, glycerol and chitosan, prevented the disintegration by imparting viscosity to ICPC.¹⁹⁻²¹ However, some suppressed the hydroxyapatite (HAP) formation and showed an inflammatory response. With a large number of hydroxyl groups, XG has the strong hydrophilicity and water retention by forming thick viscous film on the cement surface. Some studies suggested that the introduction of XG improved the injectability of ICPC but did not alter the fixation strength of screws.²²

XG is expected to prevent the fa-ICMPC from disintegration. To test our hypothesis, c-ICPC, c-ICMPC and fa-ICMPC were shaken in the deionized water for 5 min to evaluate the anti-washout property. c-ICPC was crumbled completely and powders were scattered all over the glass container once it was shaken in deionized water (Fig. 1(a)). Although some powders were escaped from the c-ICMPC initially, it remained the shape and no fine powder was fell off after shaking for 5 min (Fig. 1(b)). The difference in anti-washout property between c-ICPC and c-ICMPC is ascribed mainly to the different composition of powders. The fast setting of the MPC ameliorates the washout resistance of c-ICMPC. As shown in Fig. 1(c), fa-ICMPC not only remained the shape but also exhibited non-crumbling after shaking. Result showed that besides the effect of MPC, XG improved the anti-washout property of the fa-ICMPC significantly. When XG was dissolved in deionized water, it formed high viscosity three dimensional network structure gels and adsorbed on the surface of injectable cement. The formed viscous XG film protected the fa-ICMPC from wash-outing. The result indicated that the improved anti-washout of the fa-ICMPC contributes to broaden the clinic application, especially in highly blood perfuse regions.

Setting time and Injectability

Setting time is an important parameter for injectable cement. It is reported that the setting reaction of MPC was exothermic and accelerated the hydration process.^{5, 23-25} Beside the composition, the setting time is related to the powder to liquid ratio (P/L). Generally speaking, the shorter setting time is conducive to strengthen the anti-washout property of the cement. Previous studies showed that the fast-setting cement avoided the paste disintegration.²⁶⁻²⁷ Fig.2 presents the effect of P/L ratio and composition on the injectability and setting time of c-ICPC, c-ICMPC and fa-ICMPC. The injectability and setting time of the three cements increased significantly when the P/L ratio decreased from 2:0.8 g/mL to 2:1.4 g/mL. c-ICPC had the best injectability, followed by fa-ICMPC and c-ICMPC. The result

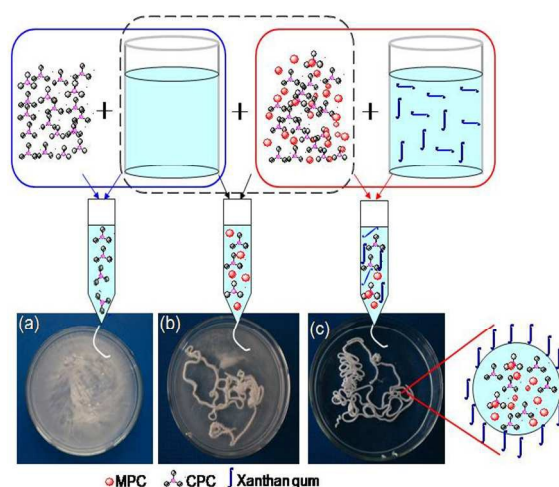


Figure 1 Anti-washout schematic diagram and the anti-washout results of injectable cement after shaking for 5 min. (a) c-ICPC, (b) c-ICMPC and (c) fa-ICMPC.

indicated that that addition of XG improved the injectability of fa-ICMPC due to its excellent rheological control.

Fig. 2 plotted that fa-ICMPC had the shortest setting time. With the increase of P/L, the setting time becomes shortened because the distance between the particles in fa-ICMPC is decreased. The result showed that MPC and XG had a synergic effect on the fa-ICMPC setting, while a shortened setting time is beneficial to improve the anti-washout property of the injectable cement. Furthermore, considering the effect of P/L ratio on injectability and setting time, the P/L ratio of 2:1.2 g/mL was chosen for further experiments.

Compressive strength

Fig.3 plots the compressive strength of the c-ICPC, c-ICMPC and fa-ICMPC after hydration for 24h. Compared with (5.80±0.84) MPa of c-ICPC, the compressive strength of the c-ICMPC is much higher and reached (13.05±0.58) MPa. This improvement is attributed to the fast setting characteristic of MPC and the increased initial mechanical strength. However, the addition of XG did not improve the compressive strength of the cement. As a hydrophilic polymer, XG in the liquid phase adsorbed deionized water, formed a high viscous gel and adsorbed on the surface of fa-ICMPC. With the main role of resistance to water, the viscous gel reduced the water into the paste to take part in the setting, which made the compressive strength of fa-ICMPC lower less than c-ICMPC. There was no statistically significant difference between c-ICMPC and fa-ICMPC in compressive strength ($p > 0.05$).

Apatite formation on the cement

The phase compositions of c-ICPC, c-ICMPC and fa-ICMPC are characterized by XRD as shown in Fig. 4. It was found that ICPC was a typical HAP structure, which had the characteristic diffraction of crystallographic planes of (002), (300), (211), (202), (310), (222), (402) and (411).²⁸ Besides HAP, magnesium phosphate ($Mg_3(PO_4)_2$) and tricalcium phosphate ($Ca_3(PO_4)_2$, TCP) were also retrieved in the hydration products

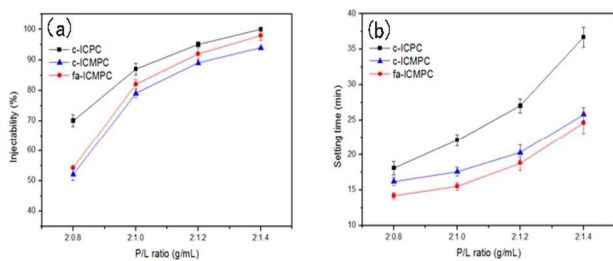


Figure 2 Effect of P/L ratios on the injectability and setting time of c-ICPC, c-ICMPC and fa-ICMPC

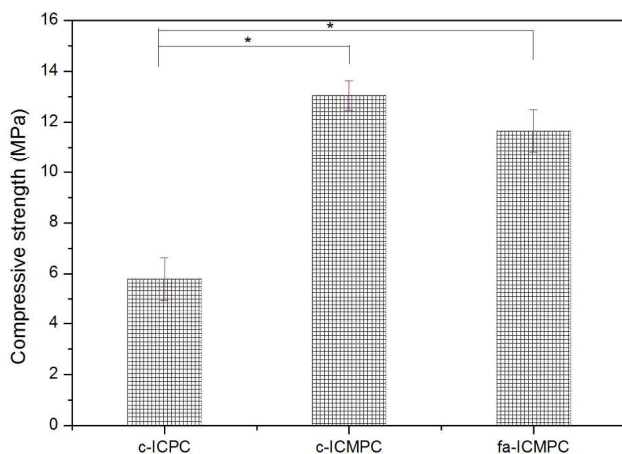


Figure 3 Compressive strength of the c-ICPC, c-ICMPC and fa-ICMPC after hydration for 24h. Statistically significant difference $p < 0.05$.

of c-ICMPC and fa-ICMPC This was in accordance with the result of Junfeng's.²⁹ The result showed that c-ICPC was hydrated to be hydroxyapatite only, while HAP, $Mg_3(PO_4)_2$ and a large amount of TCP peaks were formed on c-ICMPC and fa-ICMPC, significantly different from c-ICPC. This is due to the shifts in Ca: P ratios among these compositions.

Fig. 5 presents the typical scanning electron microscopic photographs on the fractured surface of c-ICPC, c-ICMPC and fa-ICMPC after setting for 24 h. Many crystalline particles bridged over all the cements. The hydrated c-ICPC was looser in structure compared with fa-ICMPC. The morphologies of all hydrated cements were observed clearly at a high magnification of 20000 \times . Relative small needle-like crystals, which are typical of hydroxyapatite, were covered on the c-ICPC surface. Interestingly, some lamellar-like crystals with numerous but small needle-like crystals were both fully formed on the surface of c-ICMPC and fa-ICMPC. There was no obvious difference between the fractured surfaces of c-ICMPC and fa-ICMPC, except that the crystals on c-ICMPC developed better.

Fig. 4 and Fig. 5 display the phase evolution and microstructure of the c-ICPC, c-ICMPC and fa-ICMPC. MPC and CPC were hydrated simultaneously, and the reaction equations were showed in Equation (1) and Equation (2) respectively. The result was in accordance with our previous study.³⁰

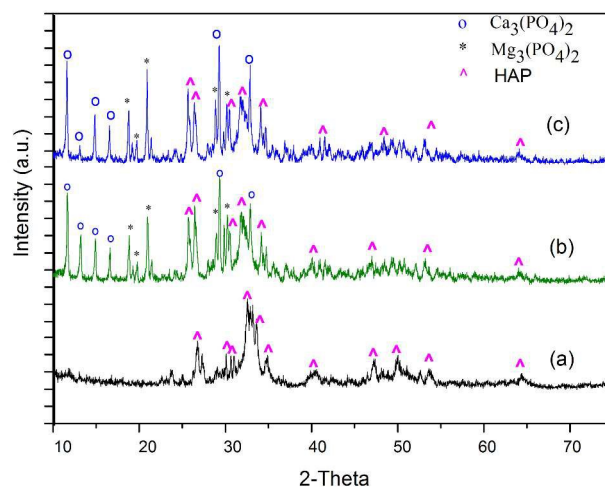


Figure 4 XRD patterns of the (a) c-ICPC, (b) c-ICMPC and (c) fa-ICMPC

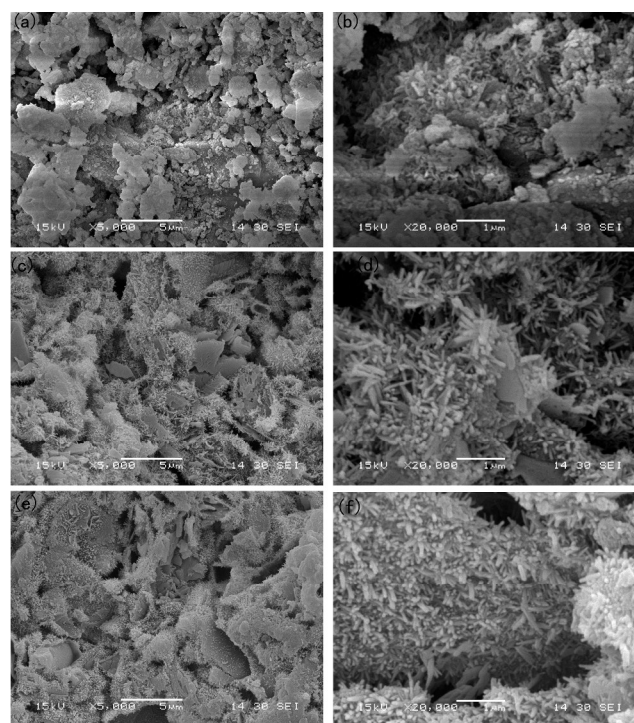
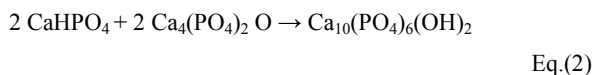
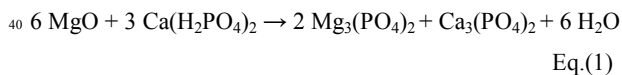


Figure 5 SEM morphologies observed in the fracture surface of ICPC and fa-ICMPC kept in an incubator at 37 $^{\circ}C$ and 100% relative humidity for 24 h : (a) c-ICPC (5000 \times), (b) c-ICPC (20000 \times), (c) c-ICMPC (5000 \times), (d) c-ICMPC (20000 \times), (e) fa-ICMPC (5000 \times) and (f) fa-ICMPC (20000 \times).



The result indicated that the addition of XG did not participate the hydration reaction of the fa-ICMPC.

Radiographic examination

Qualitative assessment of x-ray radiographs demonstrated new bone formation into fa-ICMPC (Fig.6). Strong absorption areas in dark black were observed in the defects after operation for 1 month, and the interface between fa-ICMPC and surrounding bone tissue was clear. The areas and the volumes of the fa-ICMPC were decreased with the evolution of the implantation. At month 2, the fa-ICMPC was gradually broken down into biodegradable fragments. At month 3 after implantation, absorption areas in dark black were further narrowed. Most of fa-ICMPC were biodegraded and replaced by the new bone tissue, which showed fa-ICMPC having an excellent regeneration efficacy at month 3. Radiological evaluation revealed that fa-ICMPC was not wash-outed, and filled the defects tightly and enhance the bone defect repair.

SR-CT Observation

The fa-ICMPC was injected to repair the rabbit thighbone defect. Due to its advantages in easy injectability, short setting time, good biocompatibility and improved mechanical property, ICMPC was regarded as a promising scaffold for bone regeneration.³¹ Fig.7 shows the 3D reconstruction images of the residual fa-ICMPC and the growth of new tissue after implantation for 1 month, 2 months (and 3 months by SR-CT analysis). The areas and the volumes of the fa-ICMPC decreased with the increase of the implantation time. After 1 month implantation, fa-ICMPC filled the irregular bone defect tightly and was surrounded by bone tissue. However, the interface between fa-ICMPC and the host bone was clearly visible. After 2 months, some new bone tissues formed and partially grew into fa-ICMPC. The boundary between the material and host bone was unclear due to the sufficient formation of new bone tissues. At 3 months' implantation, the fa-ICMPC continued to biodegrade and the new bone formed in many areas of the scaffold.

Histological analysis

Fig.8 and Fig.9, Fig.10 and Fig.11, Fig.12 and Fig.13 show the histological evaluation results of the c-ICMPC and fa-ICMPC implanted in the rabbit thighbones defects for 1 month, 2 months and 3 months under different magnifications (20 × and 100 ×) respectively. In masson trichrome staining, the mature bone tissue, the newly formed bone and residual material are indicated as carmine, blue, and light red or white, respectively.

After implantation for 1 month, thin trabecular new bone stained light-blue can be observed on the surfaces of c-ICMPC and fa-ICMPC (Fig.8 and Fig.9). Both c-ICMPC and fa-ICMPC were encapsulated by new bone tissues, which indicated that the new bone tissue grew from the periphery to the center. In addition, some bioresorption areas in the neighborhood of the implant surface were observed. More lipocytes were found to occupy the bioresorption area of c-ICMPC than of fa-ICMPC. The result showed that c-ICMPC had a higher degradation rate at the first month of implantation..

With the increase of the implantation up to 2 months (Fig. 10 and Fig.11), some areas were directly contacted with well-vascularized tissue. In addition, the degradation at the bone-material interface was prominent, indicating the remodeling

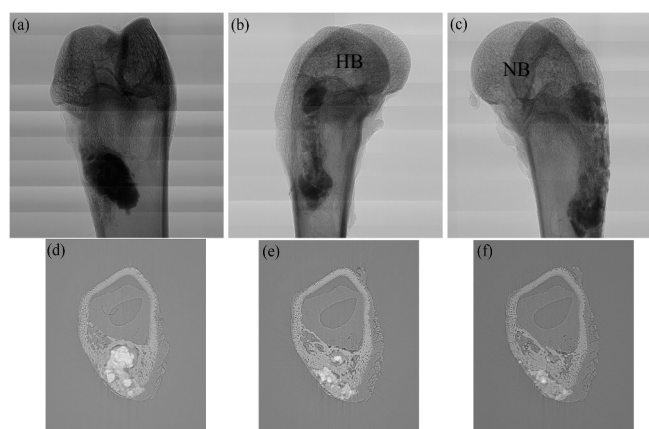


Figure 6 X-ray radiographs (a-c) and Central virtual slice(d-f) of the fa-ICMPC implanted into thighbone of rabbits at 1 month(a, d), 2 months (b, e) and 3 months (c, f). Circle shows the implanted area.

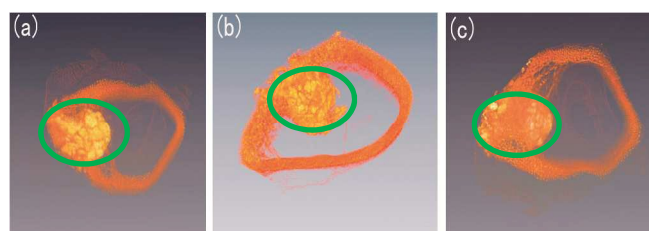


Figure 7 SR-CT image of the fa-ICMPC implanted into thighbone of rabbits at (a) 1 month, (b) 2 months and (c) 3 months. Circle shows the implanted area.

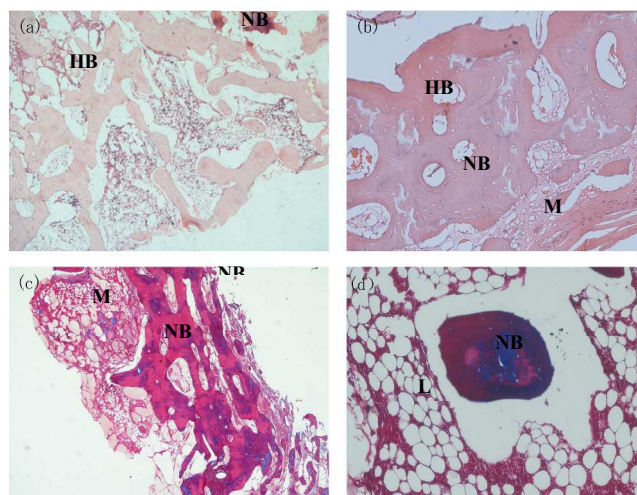


Figure 8 HE stained section ((a) 20×, (b) 100×) and Masson trichrome stained ((c) 20×, (d) 100×) after c-ICMPC implanted in vivo for 1 month. NB: newly formed bone, M: materials, HB: host bone, L: lipocytes

process of the bone.

After implantation for 3 months, almost all the surfaces of c-ICMPC and fa-ICMPC exhibited the bioresorption at different levels. The surfaces were surrounded by new immature bones (Fig. 13). The new bone in blue was rich in osteocyte lacunae and

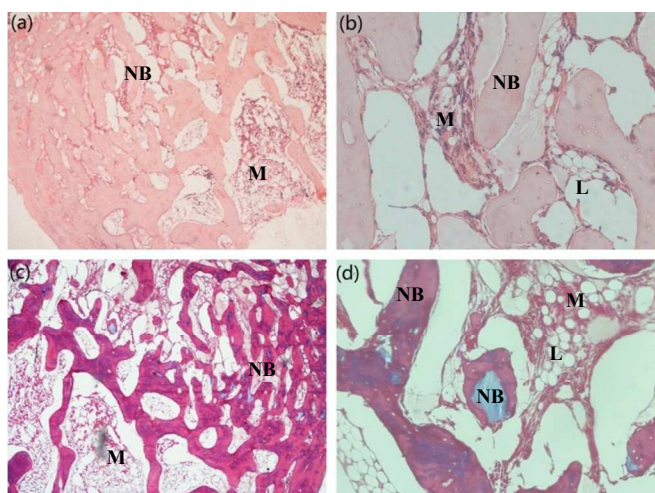


Figure 9 HE stained section ((a) 20 \times , (b) 100 \times) and Masson trichrome stained ((c) 20 \times , (d) 100 \times) after fa-ICMPC implanted in vivo for 1 month. NB: newly formed bone, M: materials, HB: host bone, L: lipocytes

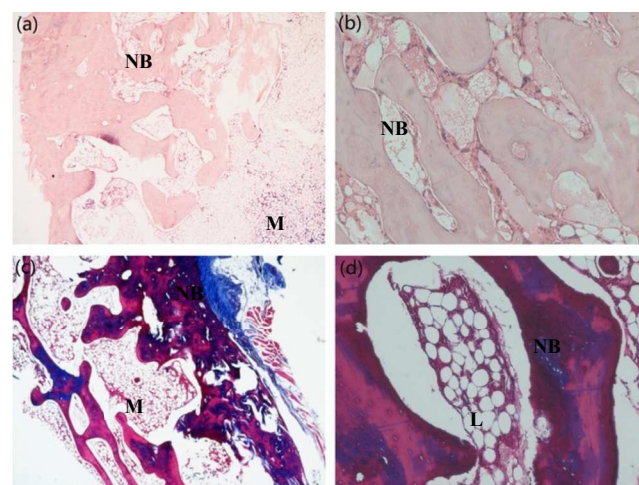


Figure 11 HE stained section ((a) 20 \times , (b) 100 \times) and Masson trichrome stained ((c) 20 \times , (d) 100 \times) after fa-ICMPC implanted in vivo for 2 months. NB: newly formed bone, M: materials, HB: host bone, L: lipocytes.

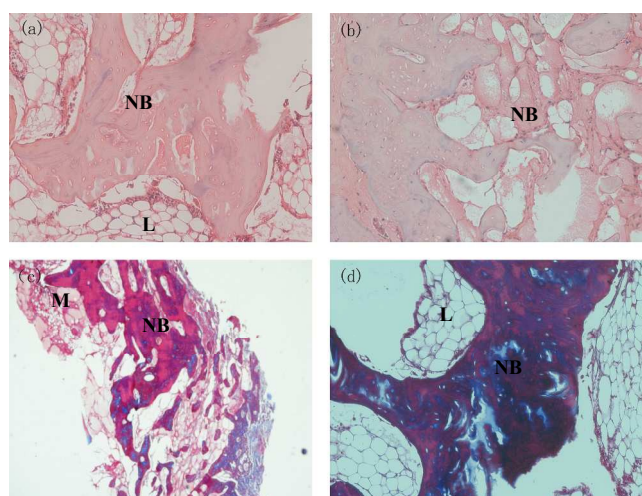


Figure 10 HE stained section ((a) 20 \times , (b) 100 \times) and Masson trichrome stained ((c) 20 \times , (d) 100 \times) after c-ICMPC implanted in vivo for 2 months. NB: newly formed bone. M: materials, HB: host bone, L: lipocytes

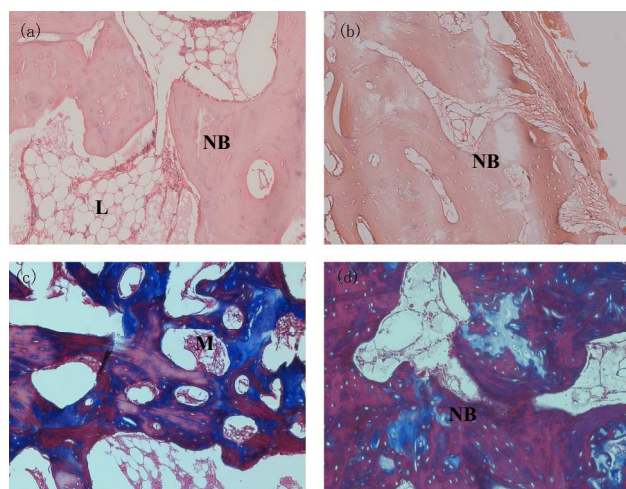


Figure 12 HE stained section ((a) 20 \times , (b) 100 \times) and Masson trichrome stained ((c) 20 \times , (d) 100 \times) after c-ICMPC implanted in vivo for 3 months. NB: newly formed bone. M: materials, HB: host bone, L: lipocytes

highly vascularized. Multinucleate giant cells and large numbers of fibroblast-like cells could be observed on the surfaces of c-ICMPC and fa-ICMPC. All these showed the formation of maturity bone tissue. No inflammatory cells or acute inflammatory processes at the surface between the tissue and the implanted materials of c-ICMPC or fa-ICMPC. In general, there is no obvious difference on the new bone formation between c-ICMPC and fa-ICMPC, except that c-ICMPC degraded faster than fa-ICMPC at the early stage of implantation.

Histomorphometrical analysis

Quantitative determination of the newly formed bone was conducted by statistical analysis of HE stained sections. Fig. 14 shows the percentage of newly formed bone in c-ICMPC and fa-ICMPC after implantation for different periods. The newly

formed bone in c-ICMPC and fa-ICMPC can both be seen to increase with the increase of the implantation periods. This may be due to the improved degradation rate of the fa-ICMPC separated by tissue embedding, thus resulted in the increase of tissue growth rate. Except at 1 month, the percentage of newly formed bone of fa-ICMPC is slightly higher than that of the c-ICMPC. After 1 month implantation, the area of newly formed bone in fa-ICMPC was about 16.5% of total area, increased to 39.9% at 2 months and further increased to 65% at 3 months. In contrast, the percentage of newly formed bone of c-ICMPC at 1 month was about 18.6%, while at 2 month and 3 months reached 35.8% and 59% respectively. The results show that the bone regenerative capacity of fa-ICMPC was just higher than that of c-ICMPC. Results in this study suggest that fa-ICMPC enhanced the short-term osteointegration property of implant, which is considered to be important for a successful

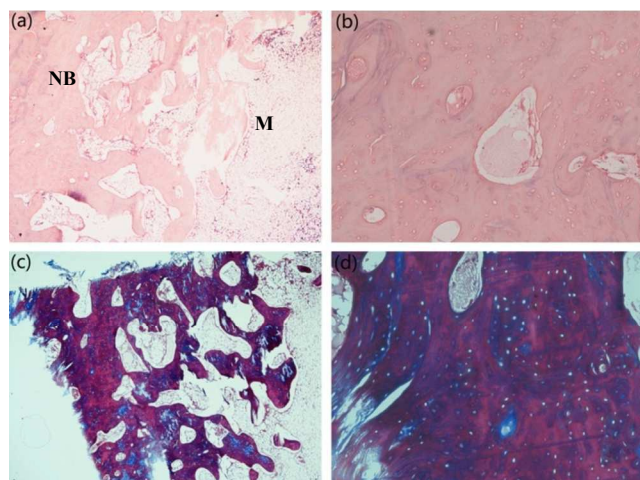


Figure 13 HE stained section ((a) 20 \times , (b) 100 \times) and Masson trichrome stained ((c)20 \times , (d) 100 \times) after fa-ICMPC implanted in vivo for 3 months. NB: newly formed bone, M: materials, HB: host bone.

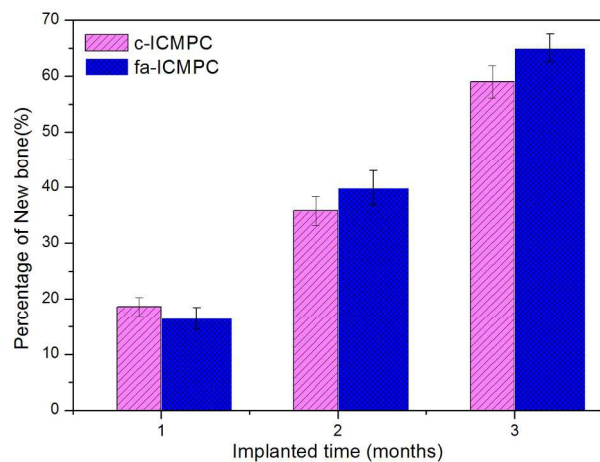


Figure 14 Quantitative analysis of the bone defect area replaced by c-ICMPC and fa-ICMPC at different implantation periods. Error bars represent means \pm SD (n = 3).

regeneration of the bone defect.

Conclusions

A fast setting and anti-washout injectable calcium–magnesium phosphate cement was developed by introducing XG and MPC into CPC. The fa-ICMPC was injected in rabbit thighbone defects to evaluate the in vivo bioresorption and bone-regenerative capacity. The result showed that the strong hydrophilicity and shape retention of XG improved the anti-washout property of fa-ICMPC while preserving its injectability. The synergistic effect of MPC and XG fastened the setting of fa-ICMPC. The fa-ICMPC was not wash-outed but biodegraded with the ingrowth of new bones in vivo. The fa-ICMPC possesses potent anti-washout property, fast setting, improved injectability, good biodegradability and osteoconductivity, and has potential application to repair the bone defects by minimally invasive treatment.

Acknowledgments

This investigation was supported by the National Basic Research Program of China (973 Program: 2012CB933600), National Natural Science Foundation of China (No. 31370960, No. 31100678), National Science and Technology Pillar Program during the Twelfth Five-years Plan Period (No. 2012BAD32B01), Program of Shanghai Leading Academic Discipline Project (No. B502), and National Special Fund for State Key Laboratory of Bioreactor Engineering (No. 2060204).

Notes and references

- [1] K. L. Low, S. H. Tan, S. H. S. Zein, J. A. Roether, V. Mourin and A. R. Boccaccini, *J. Biomed. Mater. Res., Part B*, 2010, 94(B), 273-286.
- [2] A. Chatterjea, H. P. Yuan, S. Chatterjea, H. Garritsen, A. Renard, C. A. Van Blitterswijk, J. De Boer, *Tissue Eng - Part A*, 2013, 19(3-4), 340-349.
- [3] Y. Miyamoto, K. Ishikawa, M. Takechi, Non-decay type fast-setting calcium phosphate cement: setting behavior in calf serum and its tissue response, *Biomaterials*, 1996, 17:1429-1435
- [4] T. Christel, S. Christ, J. E. Barralet, J. Groll and U. Gbureck, *J. Am. Ceram. Soc.*, 2015, 98 (3), 694-697.
- [5] C. S. Liu, Inorganic bone adhesion agent and its use in human hard tissue repair, US Patent No. 7094286B2.
- [6] F. P. Chen, C. S. Liu, J. Wei and X. L. Chen, *Int. J. Appl. Ceram. Technol.*, 2012, 9(5), 979-990.
- [7] K.J. Lilley, U. Gbureck, D.F. Farra, C. Ansell, J.E. Barralet, *J Mater Sci Mater Med* 2005, 16(4), 793-799
- [8] S. Pina, S.M. Olhero, S. Gheduzzi, A.W. Miles, J.M. Ferreira, *Acta Biomater.*, 2009, 5(5), 1233-1240
- [9] H. Izawa, S. Nishino, H. Maeda, K. Morita, S. Ifuku, M. Morimoto, H. Saimoto and J. Kadokawa, *Carbohydr. Polymers*, 2014, 8, 846-851.
- [10] M. A. Shermak, L. Wong, N. noue and T. Nicol, *J. Craniofac. Surg.*, 2000, (11), 224-31.
- [11] L. Yu, Y. Li, K. Zhao, Y.F. Tang, Z. Cheng, et al., *PLoS ONE*, 2015, 8(4), e62570.
- [12] C. S. Liu, H. F. Shao, F. Y. Chen and H. Y. Zheng, *Biomaterials*, 2006, 27, 5003-5013.
- [13] L. E. Carey, H. H. K. Xu, C. G. Simon Jr., S. Takagi and L.C. Chow, *Biomaterials*, 2005, 26, 5002-5014.
- [14] B. Han, P. W. Ma, L. L. Zhang, Y. J. Yin, K. D. Yao, F. J. Zhang, Y. D. Zhang, X. L. Li and W. Nie, *Acta Biomater.*, 2009, 5, 3165-3177.
- [15] R. A. Hugo, A. S. Luis and P. B. Carlos, *J Mater Sci: Mater Med.*, 2008, 19, 2241-2248.
- [16] S. Pina, P. M. Torres, F. Goetz-Neunhoeffler, J. Neubauer and J. M. F. Ferreira, *Acta Biomater.*, 2010, 6, 928-935.
- [17] V. Cacciafesta, M. Dalstra, C. Bosch, B. Melsen and T.T. Andreassen, *Eur J Orthod*, 2001, 23(6), 733-740.
- [18] B. R. Constantz, I. C. Ison, M. T. Fulmer, et al., *Science*, 1995, 267(5205), 1796-1799.
- [19] A. Cherng, S. Takagi, L. C. Chow, *J. Biomed. Mater. Res.*, 1997, 35, 273-277.
- [20] L. Leroux, Z. Hatim, M. Freche and J.L. Lacout, *Bone*, 1999, 25, 31S-34S.
- [21] X. P. Wang, L. Chen, H. Xiang and J. D. Ye, *J. Biomed. Mater. Res., Part B, Appl. Biomater.*, 2007, 81(B), 410-418.

- [22] P. Van. Landuyt, B. Peter, L. Beluze, et al., Bone, 1999, 25(2), 95S-98S.
- [23] E. Soudee and J. Pera, Cem. Concr. Res., 2000, 30, 315-321.
- [24] E. Soudee and J. Pera, Cem. Concr. Res., 2002, 32, 153-157.
- 5 [25] C. S. Liu, W. Gai, S. H. Pan, Z. S. Liu, Biomaterials, 2003, 24, 2995-3003
- [26] M. Z. Bellini, C. Caliari-Oliveira, A. Mizukami, K. Swiech, D. T. Covas, Donadi, E. A., P. Oliva-Neto, A. Moraes, M. Ngela, *J Biomater. Appl.*, 2015, **29(8)**, 1155-1166.
- 10 [27] E. C. Lisa, H. H. K. Xu, G. Carl, J. Simon, T. Shozo and L. C. Chow, *Biomaterials*, 2005, **26**, 5002-5014.
- [28] L. Hong, Z. Z. Guo, B. Xue, Y. M. Zhang and W.Y. Huang, *Ceram Int.*, 2011, **37(7)**, 2305-2310.
- [29] J. Jia, H. Zhou, J. Wei, X. Jiang, H. Hua, F. Chen, S. Wei
- 15 and C.S. Liu, *J R Soc Interface*, 2010, **7(49)**, 1171-1180.
- [30] F. Wu, J. Wei, H. Guo, F. P. Chen, H. Hong and C. S. Liu, *Acta Biomater.*, 2008, **4**, 1873-1884.
- [31] D. Zou, Z. Zhang, J. He, S. Zhu, S. Wang, W. Zhang and J. Zhou, *Biomaterials*, 2011, **32**, 9707-9718.

20